6th International Conference on
Protection of Structures against Hazards
16-17 October 2014, Tianjin, China

Experimental Study on Exterior Precast Concrete Frames under Column Removal Scenarios

Shaobo Kang* and Kang Hai Tan†

*School of Civil & Environmental Engineering, Nanyang Technological University
50 Nanyang Avenue, Singapore, 639798
E-mail: <skang2@e.ntu.edu.sg>

Keywords: precast concrete frames, column removal scenarios, compressive arch action, catenary action, column failure

Abstract. *With rigid boundary conditions, precast concrete beam-column sub-assemblages are capable of initiating significant compressive arch action (CAA) and catenary action under column removal scenarios. However, axial force in these bridging beams over the middle column removal may induce flexural or shear failure of adjacent side columns, which in turn hinders the full development of CAA and catenary action in beams. Thus, it is necessary to assess structural behaviour of precast concrete frames subject to column loss. This paper presents an experimental investigation on the resistance and failure mode of two precast frames. Each frame incorporates a middle beam-column joint, a double-bay beam, and two side columns. Specimens were loaded by a vertical servo-hydraulic actuator on the middle joint, and their reaction forces were recorded by a horizontal load cell on the top and a pin support at the bottom of each side column. Test results and observations indicate shear failure of the side beam-column joint, as well as bar fracture in the beam-column joint under CAA and catenary action. Conclusions from the frame tests suggest that the side columns have to be strengthened so as to protect them from potential failure under middle column removal scenarios.*

1 INTRODUCTION

In recent years, the disastrous aftermath of progressive collapse of building structures, such as the World Trade Centre in New York and the Alfred-Murrah Federal Building in Oklahoma city, has stirred up intensive research studies on the resistance of structures subject to blast loads. Accordingly, design guidelines were issued by government agencies to mitigate progressive collapse [1, 2]. Among the various design approaches against progressive collapse, the alternate path method allows local failure to occur, but seeks to arrest its disproportionate propagation through development of additional load paths, viz. CAA and catenary action, in the bridging beams over the local damage. It takes single column removal as a standard scenario by means of which the structural resistance has to be quantified experimentally or analytically.

Experimental tests on the behaviour of reinforced concrete (RC) beam-column sub-assemblages subject to column loss indicate that bridging beams are able to develop catenary action provided they have sufficient axial restraint [3-6]. However, at the frame level, mobilisation of catenary action in the beams imposes a substantially high demand on the moment resistance of side columns and the shear strength of beam-column joints, and column or joint failure may occur under combined bending moment and horizontal tension [7, 8]. Therefore, special attention has to be paid on the side columns to enable catenary action to develop in the bridging beam.

† School of Civil & Environmental Engineering, Nanyang Technological University
50 Nanyang Avenue, Singapore, 639798
E-mail: CKHTAN@ntu.edu.sg

This paper presents an experimental study on the exterior precast concrete frames under column removal scenarios, in which the side columns were only laterally restrained by load pin or load cell at the top and the bottom ends of the columns. Experimental results show that the ultimate failure of precast frames was due to fracture of the beam top reinforcement near the side columns, shear failure of the side beam-column joint or flexural failure of the side columns under catenary action, dependant on the beam reinforcement ratio.

2 EXPERIMENTAL PROGRAMME

2.1 Specimen design

Two precast concrete frames with identical dimensions were designed in accordance with Eurocode 2 [9] and scaled down to one-half model. Figure 1 shows the geometric properties of the frame. Bridging beams over the column removal and side columns were extracted from the building structure. The hatched zones represent precast beam and column units. In the precast concrete frames, precast beam and column units were prefabricated, and then the precast components were assembled into the frame with continuous longitudinal reinforcement passing through the concrete topping. In order to prevent delamination between the precast beam units and cast-in-situ concrete topping, the horizontal interface was intentionally roughened to about 3 mm and mild steel stirrups of 8 mm were provided along the beam length at 80 mm spacing.

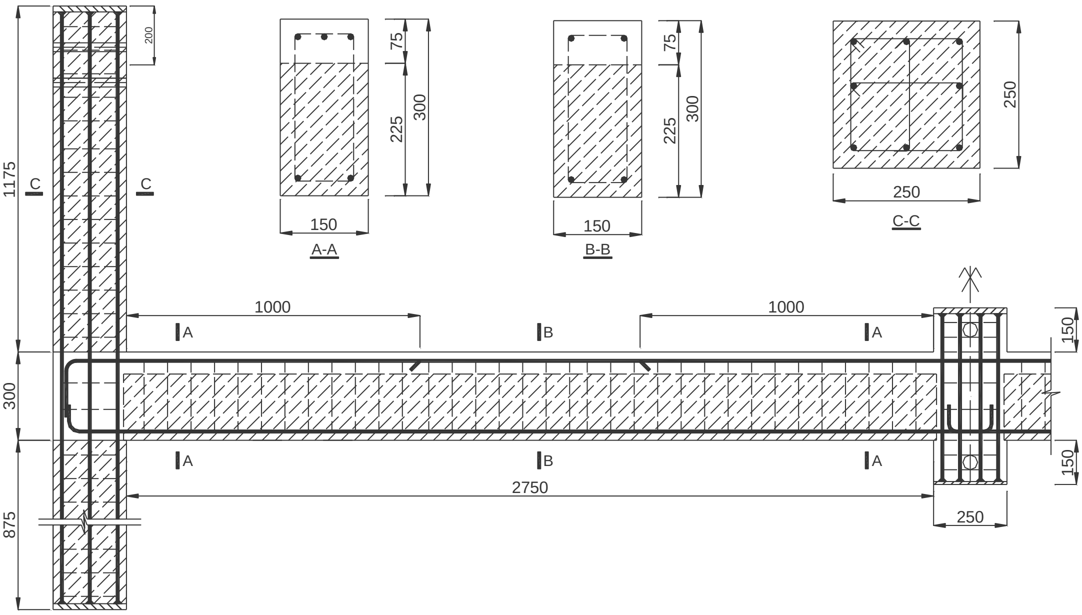

Figure 1: Geometry of Precast Concrete Frames

Specimen	Beam bars			Column bars	
	A-A	B-B	Stirrups	Main bars	Stirrups
EF-B-0.88/0.59	3T13 (top) 2T13 (bottom)	2T13 (top) 2T13 (bottom)	R8@80	8T13	R8@100
EF-B-1.19/0.59	2T16+1T13 (top) 2T13 (bottom)	2T16 (top) 2T13 (bottom)	R8@80	8T13	R8@100

Table 1: Reinforcement details of precast concrete frames

Table 1 list the reinforcement details of the precast frames. In the notations, the alphabets "EF" and "B" represent exterior frames with 90^o bend of bottom reinforcing bars in the beam-column joint, and the two numerals denote the top and the bottom reinforcement ratios at the beam section A. All other parameters of the beams and columns remained the same in the two frames except the beam top reinforcement ratio. In the beam-column joint, the diameter and spacing of stirrups remained identical to that in the column units.

2.2 Material properties

Prior to structural testing, material properties of steel reinforcement were obtained experimentally, as listed in Table 2. It is noteworthy that the steel bars at the top and bottom layers of beams were from different batches of reinforcement, and thus their nominal strengths were different. As for concrete, standard concrete cylinders with 150 mm diameter and 300 mm height were tested to obtain the compressive and splitting tensile strengths. Besides, concrete strain gauges with a gauge length of 60 mm were mounted in the middle of each cylinder to obtain its modulus of elasticity. Table 3 shows the strength and the modulus of concrete cylinders.

Material		Nominal diameter (mm)	Yield strength (MPa)	Elastic modulus (MPa)	Ultimate strength (MPa)	Fracture strain (%)	Remark
Main bars	T13	13	553.2	203895	630.8	10.8	Beam bottom bars and column bars
			593.7	202228	688.4	12.0	Beam top bars
	T16	16	493.9	204049	615.7	16.0	Beam top bars
Stirrups	R8	8	272.4	207395	359.5	--	--

Table 2: Characteristic values of steel bar properties

Specimen		Compressive strength (MPa)	Modulus of elasticity (MPa)	Splitting tensile strength (MPa)
EF-B-0.88/0.59	Precast units	27.7	22719	2.0
	In-situ concrete	26.9	25766	2.1
EF-B-1.19/0.59	Precast units	26.9	25766	2.1
	In-situ concrete	38.1	26284	2.8

Table 3: Concrete compressive and splitting tensile strengths

2.3 Test set-up and instrumentation

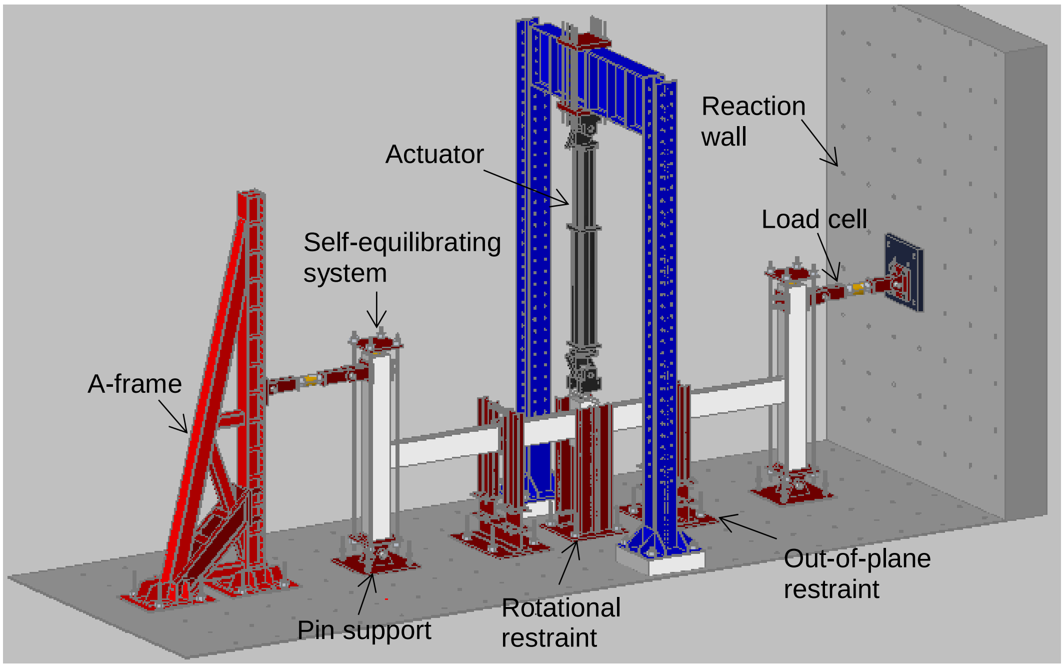

Figure 2: Test Set-up for Precast Concrete Frames

Figure 2 shows the test set-up for precast concrete frames. Underneath each side column, a pin support was fixed onto the strong floor, with a load pin inserted to capture the horizontal reaction force.

A horizontal load cell was connected to the top end of the column to constrain it from horizontal translation. In addition to the restraint system at the side column, short steel columns were employed at the mid-span of each single-bay beam to prevent its out-of-plane deflection. Rotational restraint was also utilised at the middle joint to avert its rotation after rebar fracture occurred at one side of the joint. In order to simulate axial compression force in the side column, a self-equilibrating system was fitted to the column. A flat jack was placed between the column and a thick steel plate on its top. Four steel rods were used to connect the top steel plate to the pin support at the bottom. By jacking against steel plate, compression force was imposed to the column and was equilibrated by the tension force in the four steel rods. Before testing, a stress level of $0.3f_c^{'}$ was applied onto the column, $f_c^{'}$ is the cylinder strength of concrete. Displacement-control quasi-static load was imposed on the middle joint. Corresponding vertical load and middle joint displacement were recorded by the built-in load cell of the actuator. Under column removal scenarios, sides columns to the bridging beams experienced lateral deflections when subject to CAA and catenary action [7]. Therefore, linear variable differential transducers (LVDTs) were installed along the column height to capture the lateral deflections. Figure 3 shows the layout of LVDTs.

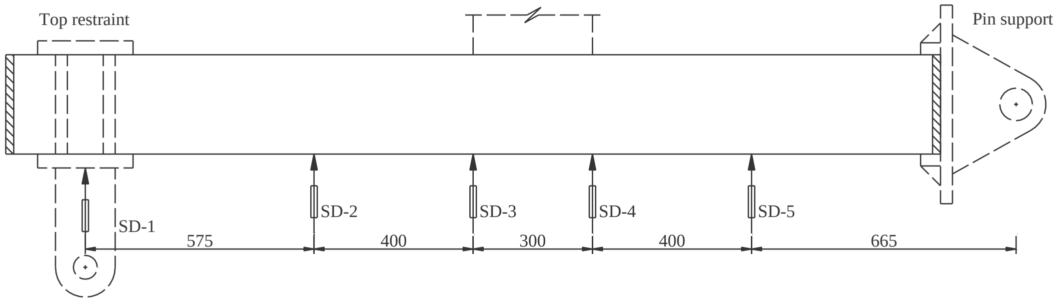

Figure 3: Layout of LVDTs along the Column Height

3 EXPERIMENTAL RESULTS

The progressive collapse resistance of exterior frames is characterised by the capacities of CAA and catenary action developed in the bridging double-bay beam under column loss scenarios. The side column plays a crucial role at the CAA and catenary action stages. Transmission of horizontal forces to the side column through the beam-column joint may induce shear failure to the joint if insufficient shear reinforcement is provided in the joint, which in turn hinders the full development of CAA and catenary action in the beam.

3.1 Load-displacement curves

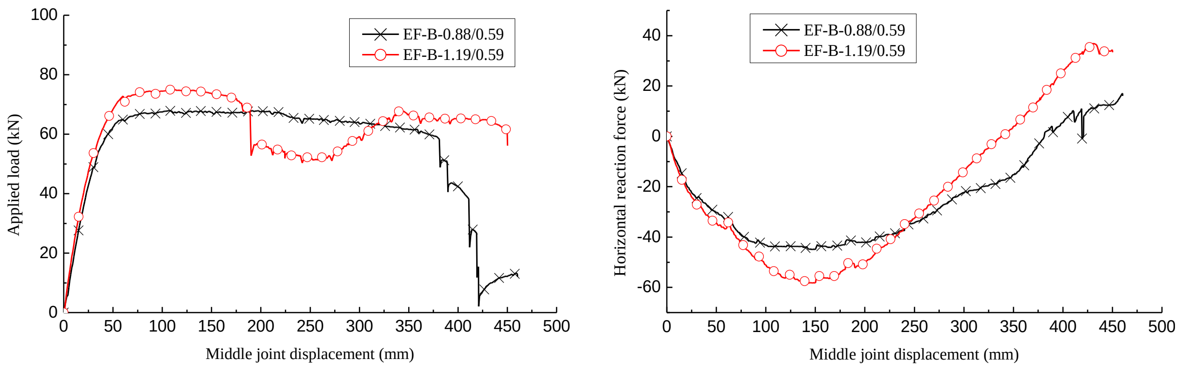

(a) Vertical Load

(b) Horizontal Reaction

Figure 4: Action-Middle Column Displacement Curves

Figures 4(a and b) show the variation of vertical load and horizontal reaction force with middle joint displacement. As defined in previous study [3, 4], CAA and catenary action feature the axial compression and tension forces in the bridging beam, respectively. Accordingly, significant CAA developed in the exterior frames at small middle column displacements. However, the comparatively smaller column showed a slow descending phase with increasing middle joint displacement. At the catenary action stage, although the horizontal reaction force in the bridging beam kept increasing, the vertical load decreased due to premature rebar fracture near the side column, or shear failure of the side beam-column joint.

Table 4 lists the CAA capacity, the peak horizontal compression force, the catenary action capacity and the maximum tension force. Compared with EF-B-0.88/0.59, the beam top reinforcement ratio of EF-B-1.19/0.59 was 35% higher, and its CAA capacity was increased by around 11% to 75.1 kN. Correspondingly, the peak compression force at the CAA stage was increased by 30% as well. After catenary action kicked in, the peak tension force in EF-B-1.19/0.59 was increased by 19.8 kN. However, the vertical load kept decreasing when the exterior frames entered into the catenary action stage. Thus, the catenary action capacity is taken as the vertical load at the onset of catenary action. Eventually, shear failure of the side joint cut off the load path of horizontal force from the bridging beam to the side column, leading to progressive collapse of EF-B-1.19/0.59. For EF-B-0.88/0.59, fracture of beam top bars near the side column induced failure.

Specimen	CAA		Catenary action	
	Capacity (kN)	Max. compression (kN)	Capacity (kN)	Max. Tension (kN)
EF-B-0.88/0.59	67.9	-45.0	51.4	17.1
EF-B-1.19/0.59	75.1	-58.3	67.7	36.9

Table 4: Capacities of Precast Concrete Frames

3.2 Failure modes

RC beam-column sub-assemblages with rigid restraints only show beam rebar rupture at the middle joint [3, 6]. Nonetheless, with 90^{o} bend of bottom bars anchored in the beam-column joint, pull-out of beam bars from the middle joint occurred in EF-B-0.88/0.59, as illustrated in Figure 5(a). However, in EF-B-1.19/0.59, one bottom bar fractured at the left face of the middle joint, leading to a drop of the vertical load in Figure 4(a), whereas the other steel bar at the left face exhibited pull-out failure, as shown in Figure 5(b). Following rebar rupture at the left face of the middle joint, the presence of rotational restraint at the middle joint enabled the moment resistance at the right face to be mobilised. Thus, the vertical load imposed on EF-B-1.19/0.59 (Figure 4(a)) could increase once again prior to the commencement of catenary action.

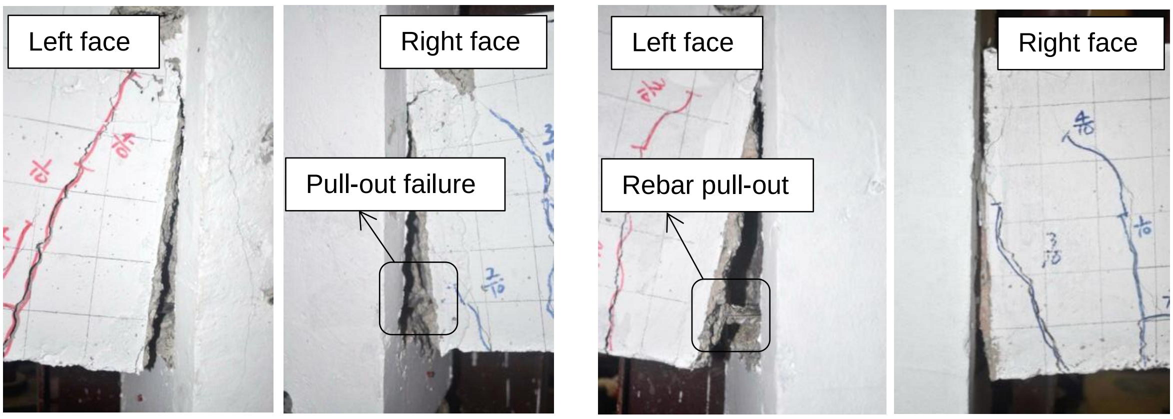

(a) EF-B-0.88/0.59 (b) EF-B-1.19/0.59

Figure 5: Failure Mode of Middle Joints

In EF-B-0.88/0.59, beam top bars near the side column fractured after the plastic hinge attained its rotational capacity, as shown in Figure 6(a). Several discrete wide cracks formed at the beam end, leading to concentration of beam rotation in the plastic hinge region. However, due to the relatively lower compression force in the beam in comparison with RC beam-column sub-assemblages [4], less severe concrete crushing was observed in the compression zone of the beam. By increasing the top reinforcement ratio in the beam of EF-B-1.19/0.59, more flexural cracks were generated in the plastic hinge region, as shown in Figure 6(b), thereby enhancing the rotational capacity of the plastic hinge. Therefore, beam bar fracture at the side column was averted. Instead, behaviour of the side column and the beam-column joint deteriorated when subject to horizontal forces produced by CAA and subsequent catenary action in the bridging beam.

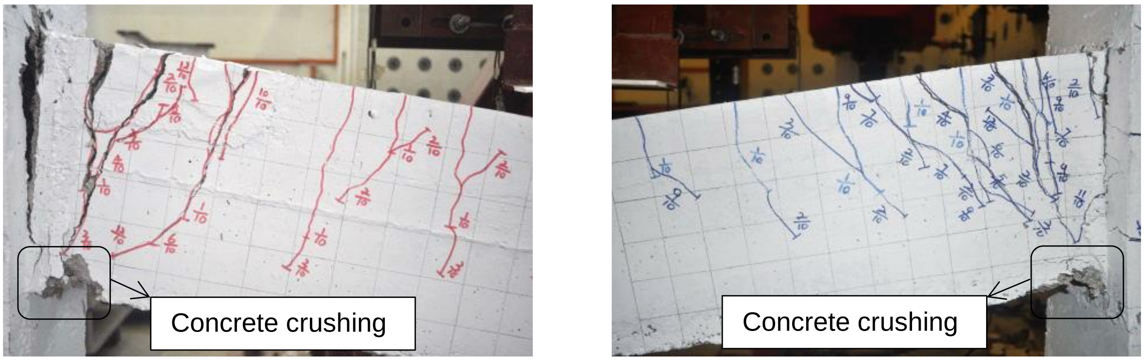

(a) EF-B-0.88/0.59 (b) EF-B-1.19/0.59

Figure 6: Failure Mode of Plastic Hinges near the Side Column

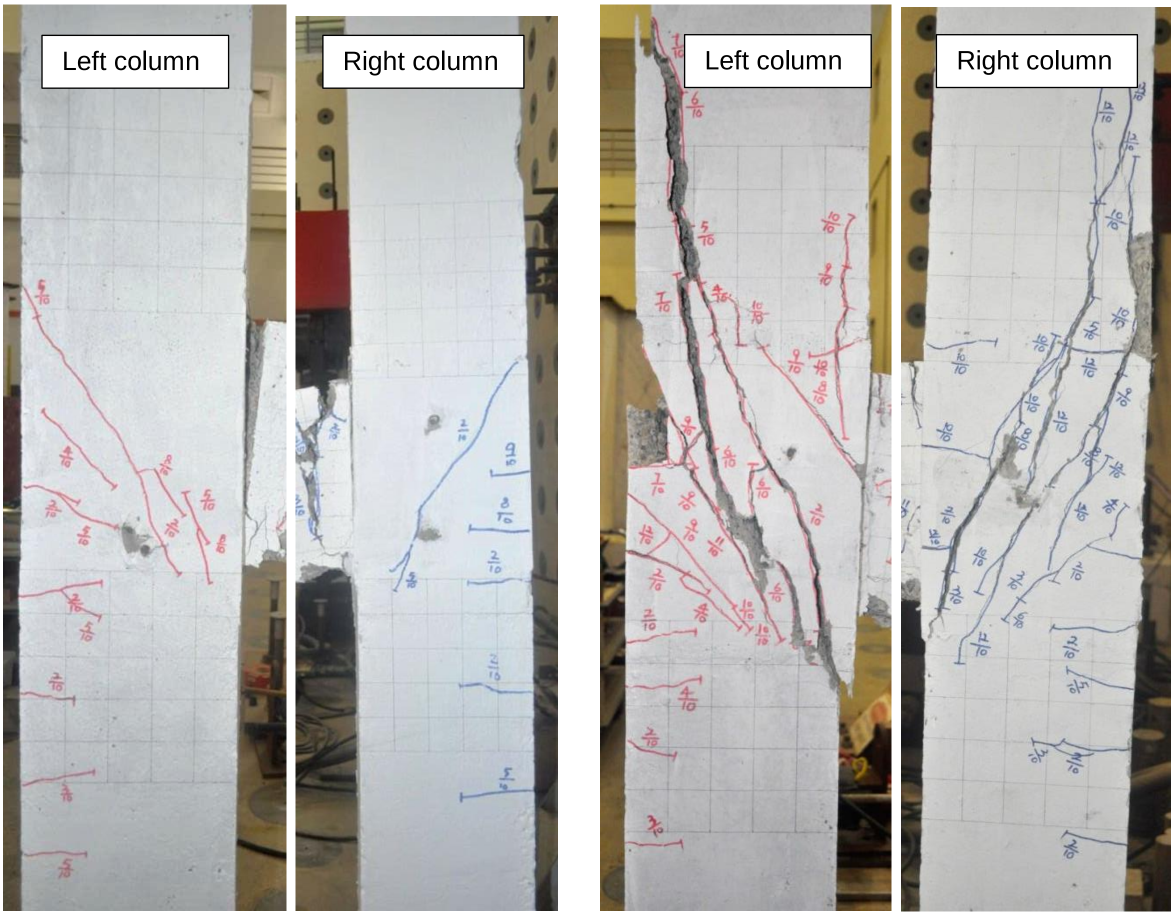

(a) EF-B-0.88/0.59 (b) EF-B-1.19/0.59

Figure 7: Failure Mode of Side Columns

Development of CAA in the bridging beam generated flexural cracks at the outer face of the column below the side beam-column joint, as shown in Figures 7(a and b), due to significant horizontal compression force acting on the column. Above the joint, little flexural cracks were observed, as compression force at the CAA stage was primarily transmitted to the pin support at the bottom of the column. Besides, diagonal shear cracks were also observed in the joint zone, especially in EF-B-1.19/0.59. This observation indicates that a higher top reinforcement ratio in the beam tends to fail the beam-column joint in the form of shear cracks. It is shear failure of the joint that cut off the load path of the horizontal force from the beam to the side column and led to decreasing vertical load at the catenary action stage. It is noteworthy that the diagonal cracks in the left joint of EF-B-1.19/0.59 were mainly formed under CAA, whereas in the right joint shear cracks developed at the catenary action stage. Therefore, beam-column joint failure occurred under both CAA and catenary action.

In addition to the total horizontal force, Figures 8(a and b) plot the reaction force in each lateral restraint on the side column. When the side column was subject to CAA, the horizontal compression force was predominantly transmitted to the bottom pin support, while the horizontal load cell at the top of the side column carried limited force. It agrees well with the crack pattern on the column, as shown in Figures 7(a and b). It is notable that the reaction in the left bottom pin support was substantially larger than that in the right support. Therefore, more severe diagonal shear cracking was observed in the left joint zone at the CAA stage, as shown in Figures 7(a and b). Following the commencement of catenary action in the bridging beam, the top load cell started to carry more tension force. In EF-B-1.19/0.59, the top load cell connected to the right column sustained much higher tension force in comparison with its counterpart at the left column, which resulted in diagonal shear cracks in the right joint at the catenary action stage, as shown in Figure 7(b). Additionally, the bottom pin support sustained almost no tension force at the catenary action stage due to shear failure of the side joint (Figure 8(b)).

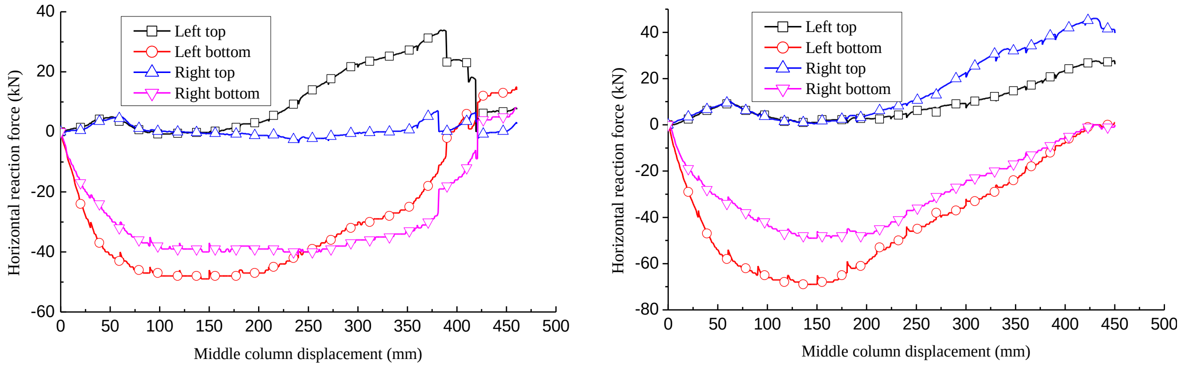

(a) EF-B-0.88/0.59 (b) EF-B-1.19/0.59

Figure 8: Reaction Forces of Lateral Restraints Connected to Side Columns

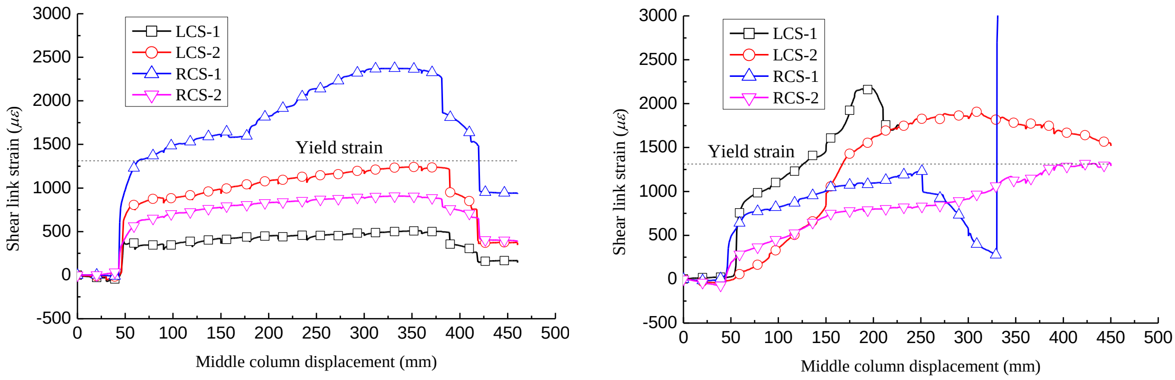

(a) EF-B-0.88/0.59 (b) EF-B-1.19/0.59

Figure 9: Strain of Shear Links in the Side Beam-Column Joint

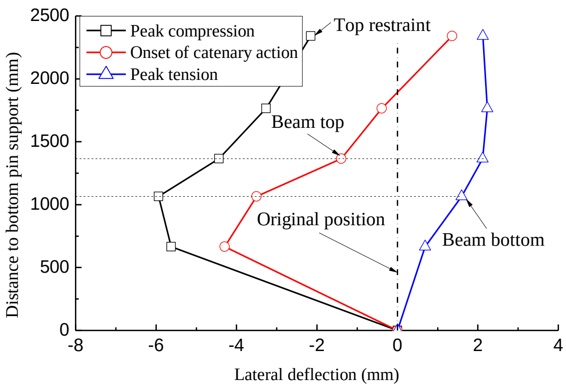

(a) EF-B-0.88/0.59

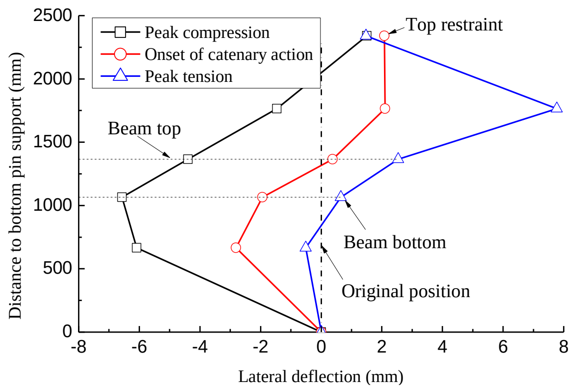

(b) EF-B-1.19/0.59

Figure 10: Lateral Deflection of the Side Column

To analyse the behaviour of the side beam-column joint, Figure 9 plots the strain of shear links in the joint zone measured by steel strain gauges. LCS-1, LCS-2, RCS-1 and RCS-2 represent the strain gauges in the left and the right side joints, respectively. Shear links in the side beam-column joint were under compression with limited compressive strains at the initial stage. When the middle joint displacement was larger than 50 mm, the strains started to increase rapidly, indicating the formation of diagonal cracks in the joint zone. Thereafter, the strain of shear links in EF-B-0.88/0.59 increased at a lower rate and remained in the elastic stage except LCS-1. Shear links were able to sustain shear force in the joint and prevented shear cracks from widening. Thus, shear failure did not occur in spite of diagonal shear cracks. However, in EF-B-1.19/0.59, shear links in the side joint entered into the post-yielding stage due to higher shear force in the joint, thereby deteriorating the shear behaviour of the side joint. Besides, diagonal shear cracking in the joint even propagated into the column above the side joint, resulting in severe spalling of concrete cover of the column.

Significant lateral deflections of the side column were recorded through LVDTs, as shown in Figure 10. The negative value denotes the deflection away from the middle joint, and the positive value stands for the deflection towards the middle joint. Under CAA, the column was pushed outwards by the horizontal compression force in the bridging beam. Similar deformed profile of the side column was obtained for EF-B-0.88/0.59 and EF-B-1.19/0.59. The maximum negative deflection up to 6 mm was attained at the column section corresponding to the bottom face of the beam. Following the onset of catenary action, inward deflection of the side column was induced due to horizontal tension force. At the catenary action stage, the column lateral deflection varied with the failure mode of the frame. Beam top bars fracture defined the progressive collapse of EF-B-0.88/0.59, with limited shear cracks in the side joint. Thus, the whole side column exhibited positive deflection, as shown in Figure 10(a). Nonetheless, shear failure of the side joint in EF-B-1.19/0.59 created a jump in the lateral deflection of the column corresponding to the beam top face. The substantially higher horizontal tension force acting on the column pulled the upper column above the side joint inwards, but load could not be transferred to the lower column due to joint failure.

4 DISCUSSIONS AND CONCLUSIONS

Under column removal scenarios, the exterior precast concrete frame EF-B-0.88/0.59 was able to develop CAA in the bridging beam. In comparison with rigid restraints, slender columns at the two ends of the beam limited the horizontal compression force due to lower stiffness and cracking at the CAA stage. Even though horizontal tension force was activated to redistribute the vertical load at large deformations, no significant catenary action was observed in the vertical load-middle column displacement curve due to premature rupture of beam top reinforcement near the side column. By increasing the beam top reinforcement ratio from 0.88% to 1.19%, a higher CAA capacity was obtained in EF-B-1.19/0.59 with slightly large horizontal compression force in the beam. Nonetheless, the side beam-column joint failed eventually instead of beam top bar fracture near the column face, which hindered the full development of catenary action in the beam.

With slender columns at the two ends of the double-bay beam, precast concrete frames may exhibit two modes of failure, viz. beam top bar fracture near the side beam-column joint and shear failure of the beam-column joint, depending on the beam top reinforcement ratio. Above all, special precaution has to be taken against shear failure of the beam-column joint under CAA and catenary action, and future experimental programme on the exterior frame is suggested to quantify the demand on shear strength of the beam-column joint under progressive collapse scenarios.

REFERENCES

[1] DOD. Design of Buildings to Resist Progressive Collapse. Unified Facilities Criteria(UFC)-4-023-03: Department of Defence, Washington, DC; 2013.
[2] GSA. Progressive Collapse Analysis and Design Guidelines for New Federal Office Buildings and Major Modernization Projects. General Services Administration, Washington, DC; 2003.
[3] Su Y, Tian Y, Song X. Progressive collapse resistance of axially-restrained frame beams. ACI Structural Journal. 2009;106:600-7.
[4] Yu J, Tan KH. Experimental study on catenary action of RC beam-column sub-assemblages. Proceedings of the 3rd *fib* International Congress 2010: Washington, DC; 2010.
[5] Yu J, Tan KH. Experimental and Numerical Investigation on Progressive Collapse Resistance of Reinforced Concrete Beam Column Sub-assemblages. Engineering Structures. 2013;55:90-106.
[6] Yu J, Tan KH. Structural Behavior of RC Beam-Column Subassemblages under a Middle Column Removal Scenario. Journal of Structural Engineering. 2013;139:233-50.
[7] Yi WJ, He QF, Xiao Y, Kunnath SK. Experimental study on progressive collapse-resistant behavior of reinforced concrete frame structures. ACI Structural Journal. 2008;105:433-9.
[8] Lew HS, Bao Y, Sadek F, Main JA, Pujol S, Sozen MA. An Experimental and Computational Study of Reinforced Concrete Assemblies under a Column Removal Scenario. NIST Technical Note 1720: National Institute of Standards and Technology, Gaithersburg, MD; 2011.
[9] BSI. Eurocode 2: Design of concrete structures—Part 1-1: General rules and rules for buildings. BS EN 1992-1-1:2004: British Standards Institution, London; 2004. p. 225.